Journal of Archaeological Science: Reports 8 (2016) 277–283

Contents lists available at ScienceDirect

Journal of Archaeological Science: Reports

journal homepage: www.elsevier.com/locate/jasrep

Cave use and palaeoecology at Maludong (Red Deer Cave), Yunnan, China

Xueping Ji [a,*], Darren Curnoe [b,*], Paul S.C. Taçon [c], Bao Zhende [d], Liang Ren [d], Raynold Mendoza [b], Haowen Tong [e], Junyi Ge [e], Chenglong Deng [f], Lewis Adler [g], Andy Baker [b], Bin Du [h]

[a] Yunnan Institute of Cultural Relics and Archaeology, Kunming, Yunnan, China
[b] Palaeontology, Geobiology and Earth Archives Research Centre, School of Biological, Earth and Environmental Sciences, University of New South Wales, Sydney, Australia
[c] Place, Evolution and Rock Art Heritage Unit, School of Humanities, Languages and Social Sciences, Gold Coast Campus, Griffith University, Queensland, Australia
[d] Mengzi Institute of Cultural Relics, Mengzi, Yunnan, China
[e] Key Laboratory of Vertebrate Evolution and Human Origins, Institute of Vertebrate Paleontology and Paleoanthropology, Chinese Academy of Sciences, Beijing, China
[f] State Key Laboratory of Lithospheric Evolution, Institute of Geology and Geophysics, Chinese Academy of Sciences, Beijing, China
[g] Bioanalytical Mass Spectrometry Facility, Mark Wainwright Analytical Centre, University of New South Wales Australia, Sydney, Australia
[h] Faculty of Tourism and Geographic Science, Yunnan Normal University, Kunming, China

ARTICLE INFO

Article history:
Received 22 April 2016
Accepted 12 June 2016

Keywords:
Human evolution
Late Pleistocene
Southwest China
Geoarchaeology
Palaeoecology

ABSTRACT

Maludong is a Terminal Pleistocene fossil-bearing cave located on the northern edge of the Southeast Asian tropical zone, southeastern Yunnan Province. Hominins from the cave include remains with affinities to archaic hominins and others with an apparent mixture of archaic and modern traits all deriving from deposits dating from the Bølling-Allerød interstadial. The sedimentary sequence of the cave appears to be largely anthropogenic in origin and records a nearly continuous record of fire lasting close to 1000 years. The fauna comprise only extant taxa and point to a rather biased sample with a preponderance of artiodactyls and carnivores, many of which show evidence for anthropogenic breakage and burning. A new analysis of the mammal fauna recovered during excavation, palaeohabitat reconstruction and stable isotope analysis of deer teeth and bones indicates the cave was located within or close to a closed forest environment. The mammal taxa also indicate a large body of water existed in the vicinity of Maludong, suggesting the modern lakes Datun Hai and Chang Qiao Hai were much larger at the time. Maludong may document an entirely novel ecological and behavioural scenario involving archaic and modern human interaction, economic exploitation and ceremonial behavior involving secondary burial practices.

1. Introduction

Maludong ('Red Deer Cave') located in southeastern Yunnan Province, Southwest China, has provided surprising insights into Late Pleistocene human evolution (Fig. 1). Excavations in 1989 provided a large sample of human remains and those published to date have aroused considerable interest on account of their morphological affinities (e.g. Boivin et al., 2013; Dennell, 2014; Bellwood, 2014; Higham, 2014; Wall, 2013). Many of the cranial and mandibular elements from the site lack the bony features widely regarded to be diagnostic of anatomically modern humans (Curnoe et al., 2012; Ji et al., 2013). Moreover, a recently described femur from Maludong shows strong size and shape resemblances to archaic humans, especially femora representing Lower Pleistocene *Homo* (Curnoe et al., 2015).

Additionally, the site has provided the first evidence for the symbolic treatment of archaic human remains in the form of ochring and the fashioning of a cranium into a strung skull vessel, which is also the oldest known example of such complex treatment of human remains globally. Bones with archaic traits from Maludong exhibit evidence for burning, cutting and ochring suggesting secondary burial practices, most parsimoniously interpreted as activities undertaken by modern humans (Ji et al., in press).

Maludong is situated within a small limestone exposure on the northern side of Huangjia Mountain, Hongzhai Village, approximately 7 km southwest of the city of Mengzi. The region containing the site is immediately (~30 km) north of the Aialo Shan-Red River shear zone, one of the great regional faults of China, mechanically associated with the transform boundary between the Indochina Block and South China Block (Leloup et al., 1995). Yunnan Province is well known for its complex topography ranging from high mountain peaks up to 6740 m through to deep valleys with altitudes well below 1000 m. Maludong is located in an area associated with relief of <1400 m and sits on the northern edge of the tropical Southeast Asian zone; its climate being most strongly affected by the Southwest and East Asian monsoons (Xiwen and Walker, 1986; Zhu et al., 2006; An et al., 2011; Li et al., 2015). Biogeographically, it is situated in one of 20 Chinese floristic centres of endemism, within a region containing high levels of

* Corresponding authors.
E-mail addresses: jxpchina@foxmail.com (X. Ji), d.curnoe@unsw.edu.au (D. Curnoe).

http://dx.doi.org/10.1016/j.jasrep.2016.06.025
2352-409X/

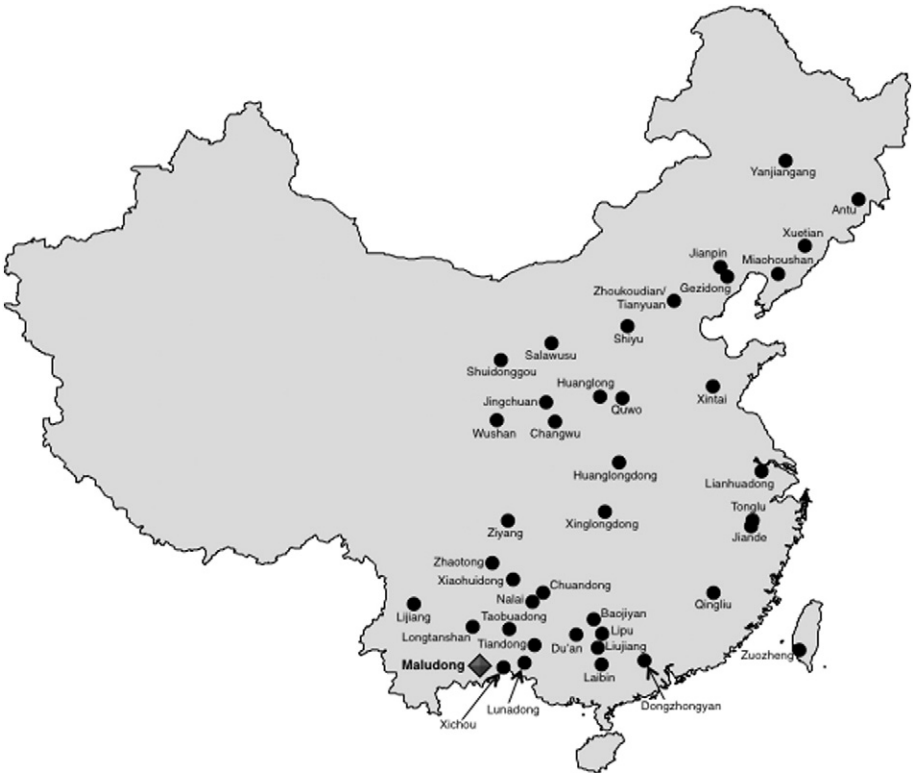

Fig. 1. Chinese Late Pleistocene hominin fossil localities.

palaeoendemism including many plant species representing relict tropical lineages that evolved with extrusion of the Indochina block to Southeast Asia (Xiwen and Walker, 1986; Hua, 2013; Li et al., 2015).

Excavations at Maludong were undertaken in 1989 by Chinese archaeologists resulting in the recovery of most of the fossils and cultural remains found at site (Zhang et al., 1991; Wu and Poirier, 1995). A small number of fossils including a human tooth were also recovered during section work in 2008 (Curnoe et al., 2012; Ji et al., 2013). New investigations of the locality and its archaeological materials began in 2008 as part of a joint Chinese-Australian project (Curnoe et al., 2012, 2015; Ji et al., 2013). In the present study, we provide new observations about the sedimentary sequence of Maludong, including data about anthropogenic cave use, and the palaeoecology of the site through a new list of mammal fauna, a palaeohabitat reconstruction and the results of stable isotope analysis on mammal bones and teeth.

2. Materials and methods

2.1. Sediments and fossils

The remaining sediments in the Maludong sequence are adhering to the eastern (rear) wall of the cave (Fig. 2). The backfill from the original excavation was removed from the locality and the sedimentary sequence was re-examined during fieldwork in 2008, 2013 and 2014. Sampling and analytical results from the 2008 work have been published previously (Curnoe et al., 2012; Ji et al., 2013), with additional research to be reported here and in future contributions.

2.2. Mammal fossils and palaeohabitat reconstruction

More than 6,000 bones and bone fragments were recovered during excavations and are held at the Mengzi Institute of Cultural Relics, Mengzi, Honghe Prefecture, Yunnan Province. Zhang et al. (1991) provided an initial faunal list for Maludong. We revise and update it here following a new investigation of the fauna during 2013.

We undertook palaeohabitat analysis on them by employing the method of Louys and Meijaard (2010). The mammalian megafauna from Maludong were first assigned to one of 14 ecological categories, developed on the basis of body size, trophic guild and locomotor type. The proportion each category represented of the total assemblage was then determined. We then used the five categories (variables) found by Louys and Meijaard (2010) to be most the effective for classifying modern ecological communities into one of three broad habitat categories ('closed', 'mixed' or 'open') in our statistical analyses. In order to standardise the data, we converted each datum to its square root. Discriminant function analysis (DFA) was then undertaken using the square root of the proportional representation data for these five variables for 25 samples from selected national parks and reserves in Asia provided by Louys and Meijaard (2010). DFA was implemented using the software IBM© SPSS© Statistics Version 23. Finally, we undertook principal component analysis (PCA) using the same five variables but for standardized proportion data from 25 Pleistocene fossil sites in Southeast Asia, also provided by Louys and Meijaard (2010). PCA was implemented using the software PAST Version 3.11 (Hammer et al., 2001).

2.3. Stable isotope analysis

Bone and tooth enamel samples were carefully individually prepared following an optimized preparation procedure (Crowley and Wheatley, 2014; Garvie-Lok et al., 2004; Koch et al., 1997). Ultrasonic cleaning was extended to 30 min following the milling of samples. Samples were treated with 30%H_2O_2 for 80 h, with evaporated losses accounted for every 12 h. After rinsing, samples were soaked in 1 M acetic acid solution (Ajax, Australia) for 4 h and rinsed. Measurement: 950–1050 μg of apatite was weighed out for each sample and analyzed on a MAT 253 isotope ratio mass spectrometer equipped with a Kiel IV carbonate device (Thermo Fisher Scientific, Bremen, Ger). Samples were reacted at 70 °C with 4 drops of 100% phosphoric acid, a reaction

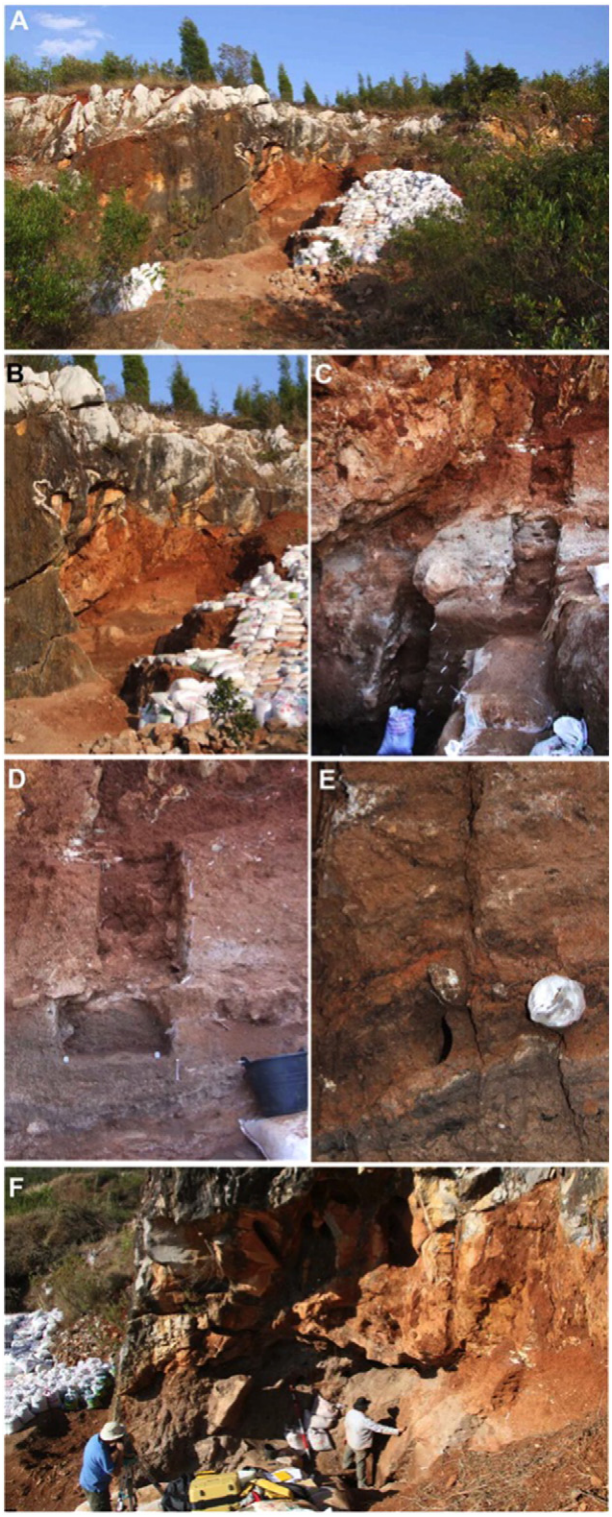

Fig. 2. Maludong locality: (A) limestone cliff containing Maludong. (B) Cave as exposed by quarrying activities showing 'witness section' in back wall (cave entrance faces west). (C) Trenches dug for sediment sampling and geochronology in 2008. (D) Upper half of Maludong sequence showing Units 1, 2 and mid-way through Unit 3 (as described herein). (E) Section detail of upper Unit 4 showing ash, apparently burnt clay and charcoal layers. (F) The cave from above where quarrying has removed the roof.

1 time of 3000 s, reaction 2 time of 120 s, with a transfer time of 90s utilized. An integration time of 16 s and 8 cycles was used.

Carbon and oxygen isotope ratios are expressed in $\delta^{13}C$ and $\delta^{18}O$ as ‰ difference in the $^{13}C/^{12}C$ and $^{18}O/^{16}O$ ratios relative to a standard reference CO_2 gas calibrated against VPDB: carbon value − 4.334 and oxygen value − 14.050 m (Thermo Fisher Scientific). Standards NBS18 and NBS19 (IAEA) were used for data correction on each day of analysis. The analytical precision of the standards was for $\delta^{13}C$ and $\delta^{18}O$ were 0.06‰ and 0.1‰ respectively.

Stable isotope measurements of carbon for a given sample are measured against a standard of known abundance. Carbon values are compared with the standard VPDB (Vienna Pee Dee Belemnite from the Cretaceous belemnite found in the Pee Dee Formation in South Carolina, also referred to as VPD and PDB) (Krigbaum, 2005). Oxygen standards can be VPBD or VSMOW (Vienna-Standard Mean Ocean Water). Results are given in delta notation (δ) and expressed as parts per thousand (‰) or "per mille" (Krigbaum, 2005). The $\delta^{13}C$ or $\delta^{18}O$ value of each sample is calculated by comparing its ratio (where R is $^{13}C/^{12}C$ or $^{18}O/^{16}O$, and A is the sample) to that of a known standard:

$$\delta A(‰) = (R\ \text{sample}/R\ \text{standard}-1) \times 1000.$$

Due to physiology, selective isotopic uptake in consumers varies by tissue type and species. Previous studies have found consistent shifts between the measured bone values and actual diet or environmental isotopes (Lai et al., 2007; Salesse et al., 2013). In order to apply the measured data to palaeodiet studies and environmental reconstructions, corrections need to be applied. Carbon studies of apatite in mammals require − 12‰ to be added to the measured stable isotope values to calculate original dietary values (Lai et al., 2007; Salesse et al., 2013).

Oxygen studies are mostly applied to palaeoclimatic and palaeodemographic studies (Hoppe, 2006; Lee-Thorp, 2008; Lopes et al., 2013). The principle underlying the use of oxygen in palaeoclimatic studies is that oxygen isotopes in the body reflect water sources. Body water has a higher measure of $\delta^{18}O$ relative to rainwater as the body preferentially loses $\delta^{16}O$. Climate and water sources can also be distinguished, as $\delta^{18}O$ values decrease with increasing latitude, altitude and distance from the coast as $\delta^{18}O$ falls in precipitation (Stuart-Williams and Schwarcz, 1997). The composition of mammalian oxygen isotope is dictated by body water. This reflects the oxygen composition that passes the specimen's body, affected by diet, physiology and environmental climate (Bryant et al., 1994; Bocherens et al., 1991; Kohn, 1996; Schoeninger et al., 2000). Oxygen isotopes, however, tend to be skewed as mammals, particularly herbivores, eat a variety of plants which have varying amounts of oxygen isotopes due to their individual water retention characteristics. The $\delta^{18}O$ was first corrected to VPDB:

$$\delta^{18}O_{VPDB} 1.14 * \delta^{18}O + 8.31$$

Followed by VSMOW correction (Stevens et al., 2011):

$$\delta^{18}O_{VSMOW} = \left(\delta^{18}O_{VPDB} * 1.03091\right) + 30.91$$

The meteoric water equivalent was calculated using the equation for red deer from Rum (Lacumin et al., 1996; Stevens et al., 2011):

$$\delta^{18}O_{rain} = \left(\delta^{18}O_{VSMOW} - 33.63\right)/0.998$$

3. Results

3.1. Sediments

Fig. 2 shows various aspects of Maludong as recorded during section work in 2008 and supplemented in 2014. A GIS plotted stratigraphic diagram and stratigraphic aggregates and details of geochronology have been published previously (see Curnoe et al., 2012; Ji et al., 2013). We provide here an updated stratigraphic division from top to bottom that includes new observations about the sediments focusing on indicators of anthropogenic activity (Table 1).

Overall, the sediments are composed of red silty clay and ash with limestone breccia inclusions. In 2008, the sedimentary sequence at Maludong was estimated to be ~3.7 m thick (Ji et al., 2013), however, with the removal of additional backfill in 2014, we have extended this to ~4.8 m. The sequence can be visually divided into six units, which incorporates the eleven sub-units described in Ji et al. (2013). Sediment accumulation rates vary markedly within and between units: Units 1–4 range ~ 0.61–0.09 m/ka, between stratigraphically defined and dated layers, but in Units 5–6 to ~0.98–0.02 m/ka. This shift likely follows the rapid transition from the Oldest Dryas (Units 6–5) to the Bølling-Allerød interstadial (Units 4–1), as suggested previously (Curnoe et al., 2012).

Interestingly, each unit in the Maludong sequence except Unit 6 contains extensive evidence for anthropogenic activity. In our previous descriptions we did not fully recognize the extent of this situation. In Units 1–5, it includes abundant charcoal and burnt fossilized animal bones, in addition to numerous combustion features in Units 2–3 (Table 1). Unit 1 is around 1.5 m thick and dates between <13,290 ± 125 cal. yr. BP and <13,720 ± 150 cal. yr. BP (see Fig. 2D, ~upper third of section). With a thickness of ~0.6 m, Unit 2 has an age of >13,720 ± 150 cal. yr. BP, contains large limestone blocks that appear to have been deliberately positioned around a hearth feature, possibly indicating the controlled use of fire in situ (Fig. 2D, ~middle third of section). These are different to the hearth features reported by Ji et al. (2013) from within the base of Unit 5, which were shown with archaeomagnetic analysis to have been heated to 250–350 °C. Also seen are apparently burnt clay deposits (Table 1).

Unit 3 is ~0.9 m thick and dates to >13,880 ± 140 cal. yr. BP to ~14,560 ± 425 cal. yr. BP. It contains numerous combustion features, charcoal, burnt and scorched fossilized bone (Fig. 2D, ~lower third of section; Table 1). All of the hominin remains were recovered from within this unit, and many of them show evidence for scorching or burning (Ji et al., in press). We have previously reported that the most complete hominin cranium from Maludong (calotte MLDG 1704) was recovered from ~15 cm below a large boulder at the top of what we are calling Unit 3. This was incorrect, as the specimen was actually found adjacent to the boulder, at about the same level as a ^{14}C date of 13,590 ± 160 cal. yr. BP on charcoal. This date is somewhat out of sequence, being 200–300 years too young in accordance with the remainder of the stratigraphy, suggesting that some mixing of younger sediments may have occurred from the middle of Unit 1 (above); although, it is within error (2*sd*) of the ^{14}C dates immediately above and below it, so random error cannot be ruled out. Unit 4 is ~0.6 m thick, dates to >14,310 ± 340 cal. yr. BP, and also contains a large quantity of charcoal as well as red consolidated clay agglomerates of likely burnt origin (Fig. 2E; Table 1).

Between Units 4 and 5 there is a ~0.2 m sterile limestone gravel unit (LSN) spanning an interval of ~2000 years. LSN seems to mark a hiatus in cave use by hominins, with an absence of sedimentation of anthropogenic origin, as is the case for the bulk of the sediments in Units 1–5. One possible cause could be a temporary closure of the cave. Unit 5 is ~0.6 m in thickness and dates between <16,630 ± 270 cal. yr. BP to >16,820 ± 185 cal. yr. BP (Table 1). It comprises red consolidated clay agglomerates of possibly burnt origin and charcoal, but with significant laminations in the gray clay and interbedded organic rich layers, indicating these deposits were probably transported for a distance from the original fireplace by water flow. Thus, Unit 5 differs from Units 1–4 in showing evidence for the transportation of sediments rather than in situ anthropogenic-associated pedogenesis. The final layer is Unit 6, a ~0.5 m thick layer of mostly dark brown clay mixed with breccia of varying size and brownish-red clay and ash. Some burnt bones were recovered during section sampling, most of which were covered by calcified sediment (Table 1).

3.2. Mammal fossils and palaeohabitat reconstruction

In Table 2 we provide a list of the identified mammal fauna recovered from Maludong. Owing to incompleteness, most fossils could only be recognized to the genus level. Three primates have been described including *H. sapiens*, an unidentified hominin represented by femur MLDG 1678 (Curnoe et al., 2015) and *Macaca*, possibly *M.* aff. *M. assamensis*, rather than the extinct *M. robustus* as proposed by Zhang et al. (1991) (see also, Ji et al., 2013). The Maludong assemblage contains an abundance of carnivore and artiodactyls, proboscideans, perissodactyls, a single lagomorph and two rodents.

DFA produced only a single component (function) and the standardized coefficients for each variable are provided in Table 3. The model was considered to be accurate, with 96.2% of cross-validated groups being correctly classified (only 1/25 sites being incorrectly classified). The cross-validated results showed Maludong to be classified as a 'closed' habitat (posterior probability: *p*0.994; 'open' *p*0.006).

Table 1
Summary of stratigraphic sequence and sedimentary indicators of possible anthropogenic activity at Maludong.

Unit	Depth (m)	Layers included[a]	Sediment description	Indicators of anthropogenic activity	Dating (cal. yr. BP, ±2σ error)[b]
1	0–1.5	BRRS, RS, LSRS (upper)	Brownish-red silty clay; small limestone breccia clasts; fossilized animal remains.	Consolidated clay agglomerates of possible burnt origin; large amount of charcoal and burnt fossilized bone.	<13,290 ± 125 to <13,720 ± 150
2	1.5–2.1	LSRS (lower), DCGA	Gray sandy silts partially capped by large limestone blocks; red consolidated clay agglomerates; fossilized animal remains.	Numerous combustion features, large quantity of charcoal, red consolidated clay agglomerates of possible burnt origin.	>13,720 ± 150
3	2.1–3.0	ORS, GAS	Brownish-red sandy silts with angular breccia of varying size up to 50 cm diameter; top to bottom, amount and size of breccia fragments decreases gradually; all hominins, and fossilized animal remains.	Numerous combustion features, charcoal, burnt and scorched fossilized bone.	>13,880 ± 140 to ~14,560 ± 425
4	3.0–3.6	ALROC, LSN	Brownish-yellow sandy silts interbedded with gray silty clay layers; some breccia appearing in small piles and bounded at its base. Angular gravels scattered through layers at random. At base of unit, a cemented sandy gravel lens with thickness ~ 20 cm (layer LSN), indicating rapid water flow.	Large quantity of charcoal, red consolidated clay agglomerates of possible burnt origin.	>14,310 ± 340
5	3.6–4.2	OROC, LGAC	Gray silty clay interbedded with black organic rich layers; fossils and stone artefacts.	Large quantity of charcoal, red consolidated clay agglomerates of possible burnt origin.	>16,630 ± 270 to >16,820 ± 185
6	4.2–4.7	BASE	Dark brown clay mixed with breccia of varying size; brownish-red clay and ash; organic slugs with clay coatings; some clay agglomerates in ball shape and coated with brown clay coatings.	Moreover, some burnt bones generally covered in hard calcified sediments have also been found during the excavation in this mixture units.	>17,830 ± 240

[a] Sedimentary layers described in Ji et al. (2013).
[b] Full details of ^{14}C dates have been reported in Curnoe et al. (2012) and Ji et al. (2013).

Table 2
Maludong mammal fauna.

Primates
Homo sapiens
Homo sp. indet.
Macaca cf. *assamensis*
Carnivora
Ursus thibetanus (G. Cuvier, 1823)
Lutra sp.
Arctonyx sp.
Panthera sp.
Viverra sp.
Canidae indet.
Proboscidea
Elephas sp.
Perissodactyl
Dicerorhinus sumatraensis (Fischer, 1814)
Artiodactyl
Sus scrofa
Moschus sp.
Axis porcinus (Zimmermann, 1780)
Elaphodus sp.
Muntiacus sp.
Naemorhedus sp.
Bos sp.
Bubalus sp.
Lagomorpha
Lepus sp.
Rodentia
Bandicota sp.
Hystrix sp.

PCA (Table 4) allowed for a comparison of Maludong with Southeast Asian Pleistocene sites, as classified using the same DFA approach by Louys and Meijaard (2010). On a plot of object scores, closed and open sites were well separated on PC1, while PC2 distinguished mixed habitat sites from those classified as closed or open (Fig. 3). Maludong was found to be unique in terms of the composition of its fauna, but plotted within the convex hull of the closed habitat sites, and outside of the range of object scores on both PCs for open and mixed habitat sites (Fig. 3).

3.3. Stable isotope analysis

The results of stable isotope analysis are presented in Table 5 and Fig. 4. There is a considerable spread in $\delta^{18}O$ meteoric values across samples with a range of 2.55‰ (min. -9.19‰, max. -11.75‰). This variability most likely reflects differences in diet, either spatial (including idiosyncratic) or temporal. Given that the provenience of the deer samples is not known we were unable to assess the importance of these factors. Furthermore, the variability found in Sample 2 is likely to be due to the sample being non-homogenous. Absolute values for $\delta^{18}O$ need to be interpreted with the caveat that the relationship between bone carbonate and meteoric water used here (Lacumin et al., 1996) derive from a different region. If the assumption is that this relationship is valid for Maludong, then meteoric water composition in the range −9.19 to −11.75‰ is comparable to modern-day wet-season rainfall at nearby Mengzi (mean $\delta^{18}O = -9.46$‰, Zhang et al., 2010). Using an isotope enabled general circulation model, Pausata et al. (2011) demonstrated that cooling during the last glacial period leads to a weakening of the Indian monsoon, with the water vapour exported from there to China being isotopically enriched. Therefore, cooler glacial conditions at Maludong would have rainfall $\delta^{18}O$ composition that is heavier than modern day values; with our bone isotope data suggestive of deposition in warm and moist interstadial conditions.

The Maludong carbon stable isotope values vary between −21.77‰ and −18.25‰, a small range of 3.52‰. All fauna sampled at this site were from a single mammalian family (Cervidae, $n = 6$). The mean standard deviation was 1.14‰. These isotope values suggest the deer sampled from Maludong fed on a strong C3 diet. C3 isotopic values display a wide range between −35‰ and −20‰, averaging −27‰ (Lai et al., 2007). The spread of the $\delta^{13}C$ may be the result of the ingestion of a range of plants by each individual deer, with the possibility also that the animals consumed plants that followed a C4 pathway.

Table 3
Standardized coefficients for variables employed in discriminant function analysis (Key: body masses: B, small; C, medium; D, large; E, very large; A, arboreal; T, terrestrial; P, primary consumer; S, secondary consumer).

Variable	Function 1	Function 2
BST	0.792	−0.032
CSA	0.602	0.204
CST	0.932	0.190
DPT	0.742	1.171
EPT	−0.894	−0.292

Table 4
Results of principal component analysis summarized for the first four components (Key: body masses: B, small; C, medium; D, large; E, very large; A, arboreal; T, terrestrial; P, primary consumer; S, secondary consumer).

	PC			
	1	2	3	4
Summary				
Eigenvalue	0.0325	0.0202	0.0189	0.0075
%-Variance	38.83	24.12	22.62	8.99
%-Cumulative	38.83	62.95	85.57	94.56
Loadings				
BST	0.7947	−0.5620	0.1146	0.1052
CSA	0.1666	0.3261	−0.5692	0.6894
CST	0.3809	0.5961	0.5749	0.2286
DPT	−0.1440	0.1507	0.4508	0.0107
EPT	−0.4182	−0.4470	0.3594	0.6792

4. Discussion

The extensive record of ash, charcoal, burnt clay and presence of hearth features and absence of obvious signs of sediment transportation

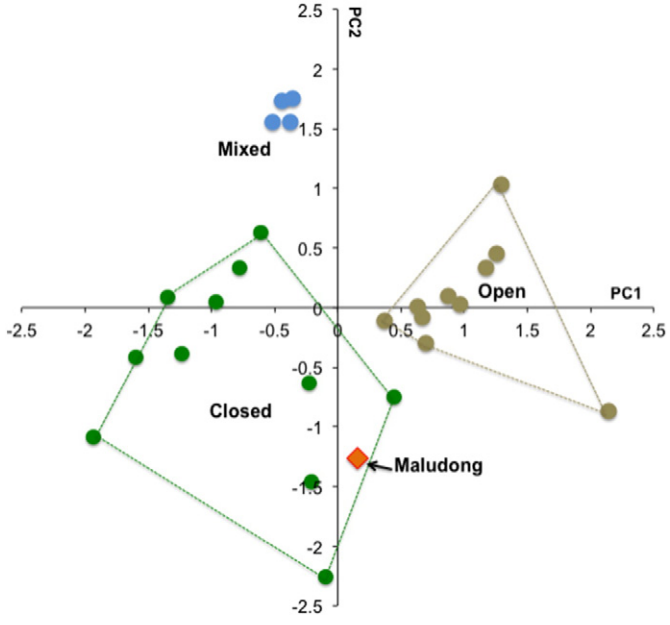

Fig. 3. Object plot from principal component analysis of five ecological categories for the megafauna from Maludong and 25 Pleistocene Southeast Asian sites.

Table 5
Results of stable isotope analysis for deer samples from Maludong.[1]

Sample	Type	$\delta^{13}C_{apatite}$	$\delta^{13}C_{VPDB}$	$\delta^{13}C_{VPDB}$ sample avg.	$\delta^{18}O_{apatite}$	$\delta^{18}O_{VPDB}$	$\delta^{18}O_{VSMOW}$	$\delta^{18}O_{rain}$	$\delta^{18}O_{rain}$ sample avg.
MLDG-SI1	Teeth	−7.95	−19.95	−19.94	−13.39	−6.95	23.74	−9.91	−9.77
MLDG-SI1 (replicate)	Teeth	−7.93	−19.93		−13.15	−6.68	24.02	−9.63	
MLDG-SI2	Teeth	−8.19	−20.19	−19.87	−13.81	−7.44	23.24	−10.41	−10.74
MLDG-SI2 (replicate)	Teeth	−7.54	−19.54		−14.38	−8.08	22.58	−11.07	
MLDG-SI4	Long bone	−8.98	−19.92	−19.92	−14.93	−8.71	21.93	−11.72	−11.72
MLDG-SI6	Long bone	−6.25	−18.25	−18.30	−14.96	−8.74	21.90	−11.75	−11.63
MLDG-SI6 (replicate)	Long bone	−6.35	−18.35		−14.75	−8.50	22.14	−11.51	
MLDG-SI7	Long bone	−9.77	−21.77	−21.72	−12.94	−6.44	24.27	−9.38	−9.29
MLDG-SI7 (replicate)	Long bone	−9.67	−21.67		−12.78	−6.26	24.45	−9.19	
MLDG-SI8	Long bone	−8.87	−20.87	−20.87	−14.70	−8.44	22.21	−11.44	−11.44
S.D.				1.15					1.03

[1] Equations used to correct the $\delta^{18}O$ values of VPDB, VSMOW, and meteoric water were taken from Stevens et al. (2011).

leads us to interpret Units 1–4 of the Maludong cave sedimentary sequence as evincing a near-continuous record for the use of fire lasting >1000 years. We suggest that the fireplaces gradually moved into the cave perhaps due to cave collapse and rapid accumulation of sediment at the entrance place as suggested by a sharp increase in the accumulation rates of deposits between about 14.3 ka and 13.3 ka. The older deposits (Units 5–6) show evidence of lamination and water deposition such that ash, charcoal and other fire-derived materials were likely to have been transported from towards the entrance to the back of the cave along a slope.

Overall, the mammal fauna from Maludong lacks extinct taxa and points to a rather biased sample with a preponderance of carnivores and artiodactyls, especially deer taxa. Many of the fauna, especially the deer, also show evidence for deliberate breakage and burning indicating that their presence in the Maludong sediments is best explained by anthropogenic factors. This would suggest a rather diverse diet for the hominins utilizing Maludong, predominantly graminivorous, and possibly also carnivorous taxa, although, a taphonomic analysis of the fauna is presently underway and will further assess evidence for the economic use of the various taxa. The major challenge with reconstructing palaeoecology from the fauna at Maludong is the absence of records about where individual fossils were recovered from within the stratigraphic sequence. Although the time interval covered by the Maludong sequence is not especially long (~4540 years), it spans both the Older Dryas and Bølling-Allerød interstadial, and so potentially documents at least one major palaeoecological shift in China during the Late Pleistocene (Wang et al., 2008). However, as most of the fossils recovered during the 1989 excavations are derived from Units 1–4, spanning just over 1000 years, the palaeoecological signal we analyse here at Maludong is from the Bølling-Allerød interstadial.

Some of the fauna provide insights into the broad palaeoecology of Maludong and its surrounding environment. Species of the deer genus *Mochus* mostly inhabit forested regions in Asia (IUCN, 2015), while *Axis porcinus* was known historically to inhabit the lowest valleys of Xishuangbanna, a tropical rainforest region in southwest Yunnan

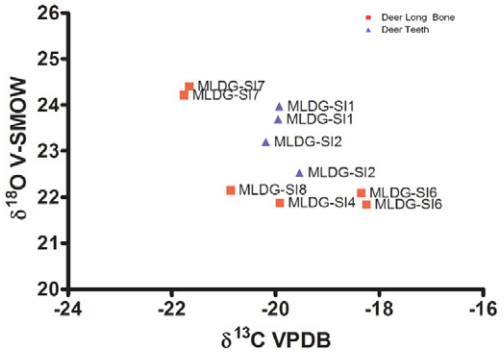

Fig. 4. Stable isotope results from deer tooth enamel and bone from Maludong.

(Ohtaishi and Gao, 1990; Smith and Xie, 2008). Moreover, this species is today generally known to inhabit wet or moist tall grasslands often associated with medium- to large-sized rivers (Bhowmik et al., 1999; Biswas and Mathur, 2000; Biswas, 2004). *Elaphodus* is today also found in mountainous forested regions close to water (Ohtaishi and Gao, 1990). The otter (genus *Lutra*) is associated with a wide variety of aquatic habitats, including highland and lowland lakes, rivers, streams, marshes and swamp forests (Mason and Macdonald, 1986). The Asiatic black bear (*Ursus thibetana*) is known to occupy a variety of forested habitats, both broad-leaved and coniferous types (IUCN Red List, 2015), while the Sumatran rhinoceros (*Dicerorhinus sumatraensis*) inhabits tropical rainforest and montane moss forest, and occasionally occurs at forest margins and in secondary forest, mainly in hilly areas nearby to water sources (Nowak, 1999).

The presence of all of these taxa suggests a considerable body of water in the vicinity of Maludong. As the immediate area around the locality today lacks obvious evidence for a recent river or palaeodrainage channel, these species may signal much larger bodies of water such as those associated with a Pleistocene extension of the nearby lakes Datun Hai and Chang Qiao Hai, presently located 8–9 km to the northwest and northeast of Maludong. Moreover, it seems likely that the region contained forested habitats, probably tropical monsoon forest, as seen more broadly in the region today (Li et al., 2015), as well as a component of wet grassland elements, perhaps associated with adjacent lakes. Such a reconstruction is confirmed by our palaeohabitat analysis, which classified the Maludong mammal fauna as representing a 'closed' habitat (e.g. DF $p0.994$).

Oxygen and carbon stable isotopes from deer enamel and bones provide additional insights into the palaeoenvironmental context of the site. The bone oxygen isotope values, when corrected to a rainwater equivalent, are similar to modern day wet-season rainfall composition, being isotopically lighter than the modern-day annual mean rainfall of the region (Zhang et al., 2010). This would indicate that interstadial conditions, possibly wetter than today, prevailed at the time that sediments were formed. This is consistent with the fauna and sediment evidence, in the form of geochronological, sedimentological and archaeomagnetic data, for deposition during the Bølling-Allerød interstadial (see also Curnoe et al., 2012; Ji et al., 2013). Stable carbon isotope values indicate that the deer sampled in the present study likely fed on a strongly C3 based diet. C3 plants include most trees, herbs, shrubs, shady grasses, rice, all tubers, fruits, nuts and most vegetables, including all rainforest flora, and they dominate temperate latitudes (Krigbaum, 2005; Lai et al., 2007). This includes many of the dietary items of the extant representatives of the deer taxa represented at Maludong, although, all of them are known to consume a wide variety of foods including C4 items (e.g. see Ohtaishi and Gao, 1990; IUCN, 2015). Thus, the results of carbon stable isotope analysis are consistent with palaeoecological interpretations based on the faunal list and palaeohabitat classification using modern analogues, namely, that Maludong was likely to have been within or located close to a forested

environment. Although a preliminary analysis of sediments in 2010 failed to reveal the presence of plant remains (D. Penny, Pers. Comm.), more comprehensive palaeobotanical work is currently underway and should allow a further test of this reconstruction.

5. Conclusion

Little is known at present about the environmental use, economic behavior and palaeoecology of Late Pleistocene humans in southern China. Maludong in southeastern Yunnan provides the only example in the region documenting extensive anthropogenic cave use involving economic and ritual behavior as shown by taphonomic markers on faunal skeletal elements, modified human remains and extensive evidence for fire including a near-continuous record of fire spanning >1000 years. Other hominin-bearing Late Pleistocene caves in southern China would seem only to contain fossils and cultural materials within natural sedimentary accumulations (see Wu and Poirier, 1995). Importantly also is the presence of human remains with archaic morphology at Maludong, which indicates the sympatry in this region of late surviving archaic hominins and modern humans and reveals evidence for ecological/economic interactions between them. The multi-proxy palaeoecological evidence presented here suggests that Maludong was located within or close to a closed, tropical forest, similar to that seen in the southern parts of Yunnan today. This also makes Maludong the only example on mainland East Asia of the Pleistocene human occupation of a closed habitat – although we note several examples from Southeast Asia (e.g. Storm et al., 2005; Piper and Rabett, 2009; Hunt et al., 2012) – and the only one we know of implying forest inhabitation by archaic humans; another possibility being the Lower Pleistocene locality of Kedung Brubus in Java (see Louys and Meijaard, 2010).

Acknowledgements

This research was primarily funded by Australian Research Council grants DP0877603 and FT120100168 and Yunnan Institute of Cultural Relics and Archaeology grant A-201301.

References

An, Z.S., Clemens, S.C., Shen, J., Qiang, X.K., Jin, Z.D., Sun, Y.B., Prell, W.L., Luo, J.J., Wang, S.M., Xu, H., Cai, Y.J., Zhou, W.J., Liu, X.D., Liu, W.G., Shi, Z.G., Yan, L.B., Xiao, X.Y., Chang, H., Wu, F., Ai, L., Lu, F.Y., 2011. Glacial-interglacial Indian summer monsoon dynamics. Science 333, 719–723.

Bellwood, P., 2014. First Migrants: Ancient Migration in Global Perspective. John Wiley & Sons.

Bhowmik, M.K., Chakraborty, T., Raha, A.K., 1999. The habitat and food habits of hog deer (*Axis porcinus*) in protected areas of sub-Himalayan West Bengal. Tiger Paper 26, 25–27.

Biswas, T., 2004. Hog deer (*Axis porcinus* Zimmerman, 1780). ENVIS Bull. 7, 61–78.

Biswas, T., Mathur, V.B., 2000. A review of the present conservation scenario of hog deer (*Axis porcinus*) in its native range. Indian For. 126, 1068–1084.

Bocherens, H., Fizet, M., Mariotti, A., Lange-Badre, B., Vandermeersch, B., Borel, J.P., Bellon, G., 1991. Isotopic biogeochemistry (^{13}C,^{15}N) of fossil vertebrate collagen: application to the study of a past food web including Neandertal man. J. Hum. Evol. 20, 481–492.

Boivin, N., Fuller, D.Q., Dennell, R., Allaby, R., Petraglia, M.D., 2013. Human dispersal across diverse environments of Asia during the Upper Pleistocene. Quat. Int. 300, 32–47.

Bryant, J.D., Luz, B., Froelich, P.N., 1994. Oxygen isotopic composition of fossil horse tooth phosphate as a record of continental paleoclimate. Palaeogeogr. Palaeoclimatol. Palaeoecol. 107, 303–316.

Crowley, B.E., Wheatley, P.V., 2014. To bleach or not to bleach? Comparing treatment methods for isolating biogenic carbonate. Chem. Geol. 381, 234–242.

Curnoe, D., Ji, X., Herries, A.I.R., Kanning, B., Taçon, P.S.C., Zhende, B., Fink, D., Yunsheng, Z., Hellstrom, J., Yun, L., Cassis, G., Su, B., Wroe, S., Shi, H., Parr, W.C.H., Shengmin, H., Rogers, N., 2012. Human remains from the Pleistocene-Holocene transition of Southwest China suggest a complex evolutionary history for east Asians. PLoS One 7, e31918.

Curnoe, D., Xueping, J., Wu, L., Bao, Z., Taçon, P.S.C., Liang, R., 2015. An archaic hominin femur from the Late Pleistocene of Southwest China. PLoS One 10, e0143332.

Dennell, R., 2014. Smoke and mirrors: the fossil record for *Homo sapiens* between Arabia and Australia. In: Dennell, R., Porr, M. (Eds.), Southern Asia, Australia and the Search for Human Origins. Cambridge University Press, Cambridge, pp. 33–50.

Garvie-Lok, S.J., Varney, T.L., Katzenberg, M.A., 2004. Preparation of bone carbonate for stable isotope analysis: the effects of treatment time and acid concentration. J. Archaeol. Sci. 31, 763–776.

Hammer, Ø., Harper, D.A.T., Ryan, P.D., 2001. PAST: paleontological statistics software package for education and data analysis. Palaeontol. Electron. 4 (9 pp.).

Higham, C., 2014. Early Mainland Southeast Asia. River Books, Bangkok.

Hoppe, K.A., 2006. Correlation between the oxygen isotope ratio of North American bison teeth and local waters: implication for paleoclimatic reconstructions. Earth Planet. Sci. Lett. 244, 408–417.

Hua, Z., 2013. The floras of southern and tropical southeastern Yunnan have been shaped by divergent geological histories. PLoS One, e64213.

Hunt, C.O., Gilbertson, D.D., Rushworth, G., 2012. A 50,000-year record of late Pleistocene tropical vegetation and human impact in lowland Borneo. Quat. Sci. Rev. 37, 61–80.

IUCN, 2015. The IUCN red list of threatened species. Version 2015.2. http://www.iucnredlist.org (Downloaded on 27 July 2015).

Ji, X., Curnoe, D., Bai, K., Herries, A., Bao, Z., Fink, D., Luo, Q., Helstrom, J., Zhu, Y., Hellstrom, J., Luo, Y., Taçon, P.S.C., 2013. Further geological and paleoanthropological investigations at the Maludong hominin site, Yunnan Province, Southwest China. Chin. Sci. Bull. 58, 4472–4485.

Koch, P.L., Tuross, N., Fogel, M.L., 1997. The effects of sample treatment and diagenesis on the isotopic integrity of carbonate in biogenic hydroxylapatite. J. Archaeol. Sci. 24, 417–429.

Kohn, M.J., 1996. Predicting animal ^{18}O: accounting for diet and physiological adaptation. Geochim. Cosmochim. Acta 60, 4811–4829.

Krigbaum, J., 2005. Reconstructing human subsistence in the West Mouth (Niah Cave, Sarawak) burial series using stable isotopes of carbon. Asian Perspect. 44, 73–89.

Lacumin, P., Bocherens, H., Mariotti, A., Longinelli, A., 1996. Oxygen isotope analyses of coexisting carbonate and phosphate in biogenic apatite: a way to monitor diagenetic alteration of bone phosphate? Earth planet. Sci. Lett. 142, 1–6.

Lai, L., Tykot, R.H., Beckett, J.F., Floris, R., Fonzo, O., Usai, E., Manunza, M.R., Goddard, E., Hollander, D., 2007. Interpreting stable isotopic analyses: case studies on Sardinian prehistory. In: Glascock, M.D., Speakman, R.J., Popelka-Filcoff, R.S. (Eds.), Archaeological Chemistry: Analytical Techniques and Archaeological Interpretation, pp. 114–136 (Washington, DC).

Lee-Thorp, J.A., 2008. On isotopes and old bones. Archaeometry 50, 925–950.

Leloup, P.H., Lacassin, R., Tapponnier, P., Schärer, U., Zhong, D., Liu, X., Zhang, L., Ji, S., Trinh, P.T., 1995. The Ailao Shan-Red River shear zone (Yunnan, China), tertiary transform boundary of Indochina. Tectonophysics 251, 3–84.

Li, R., Kraft, N.J., Yang, J., Wang, Y., 2015. A phylogenetically informed delineation of floristic regions within a biodiversity hotspot in Yunnan, China. Sci. Rep. 5, 9396.

Lopes, R.P., Ribeiro, A.M., Dillenburg, S.R., Schultz, C.L., 2013. Late middle to late Pleistocene paleoecology and paleoenvironments in the coastal plain of Rio Grande do Sul State, Southern Brazil, from stable isotopes in fossils of Toxodon and Stegomastodon. Palaeogeogr. Palaeoclimatol. Palaeoecol. 369, 385–394.

Louys, J., Meijaard, E., 2010. Palaeoecology of Southeast Asian megafauna-bearing sites from the Pleistocene and a review of environmental changes in the region. J. Biogeogr. 37, 1432–1449.

Mason, C.F., Macdonald, S.M., 1986. Otters: Ecology and Conservation. Cambridge University Press, Cambridge.

Nowak, R.M., 1999. Walker's Mammals of the World. The John Hopkins University Press, London.

Ohtaishi, N., Gao, Y.T., 1990. A review of the distribution of all species of deer (Tragulidae, Moschidae and Cervidae) in China. Mammal Rev. 20, 125–144.

Pausata, F.S.R., Battisti, D.S., Nisancioglu, K.H., Bitz, C.M., 2011. Chinese stalagmite δ18O controlled by changes in the Indian monsoon during a simulated Heinrich event. Nat. Geosci. 4, 474–479.

Piper, P.J., Rabett, R.J., 2009. Hunting in a tropical rainforest: evidence from the Terminal Pleistocene at Lobang Hangus, Niah Caves, Sarawak. Int. J. Osteoarchaeol. 19, 551–565.

Salesse, K., Dufour, É., Castex, D., Velemínský, P., Santos, F., Kuchařová, H., Jun, L., Brůžek, J., 2013. Life history of the individuals buried in the St. Benedict Cemetery (Prague, 15th–18th Centuries): insights from ^{14}C dating and stable isotope ($\delta^{13}C$, $\delta^{15}N$, $\delta^{18}O$) analysis. Am. J. Phys. Anthropol. 151, 202–214.

Schoeninger, M.J., Kohn, M.J., Valley, J., 2000. Tooth oxygen isotope ratios as palaeoclimate monitors in arid ecosystems. In: Katzenberg, M.A., Ambrose, S.H. (Eds.), Biogeochemical Approaches to Palaeodietary Analysis. Kluwer Academic/Plenum Publishers, New York, pp. 117–140.

Smith, A.T., Xie, Y. (Eds.), 2008. A Guide to the Mammals of China. New Jersey Princeton University Press, Princeton.

Stevens, R.E., Balasse, M., O'Connell, T.C., 2011. Intra-tooth oxygen isotope variation in an known population of red deer: implications for past climate and seasonality reconstructions. Palaeogeogr. Palaeoclimatol. Palaeoecol. 301, 64–74.

Storm, P., Aziz, F., de Vos, J., Kosasih, D., Baskoro, S., van den Hoek Ostende, L.W., 2005. Late Pleistocene *Homo sapiens* in a tropical rainforest fauna in East Java. J. Hum. Evol. 49, 536–545.

Stuart-Williams, H.L.Q., Schwarcz, H.P., 1997. Oxygen isotopic determination of climatic variation using phosphate from beaver bone, tooth enamel, and dentine. Geochim. Cosmochim. Acta 61, 2539–2550.

Wall, J.D., 2013. Great ape genomics. ILAR J. 54, 82–90.

Wang, Y., Cheng, H., Edwards, R.L., Kong, X., Shao, X., Chen, S., Wu, J., Jiang, X., Wang, X., An, Z., 2008. Millennial-and orbital-scale changes in the East Asian monsoon over the past 224,000 years. Nature 451, 1090–1093.

Wu, X., Poirier, F., 1995. Human Evolution in China. Oxford University Press, Oxford.

Xiwen, L., Walker, D., 1986. The plant geography of Yunnan Province, Southwest China. J. Biogeogr. 13, 367–397.

Zhang, X., Zheng, L., Yang, L., Bao, Z., 1991. Human fossils and the paleoculture from Mengzi. In: Yunnan Provincial Museum (Ed.), On Materials of Human Origin and Prehistoric Culture of Yunnan. Yunnan Renming Press, Kunming, pp. 234–246 (in Chinese).

Zhang, X.-P., Liu, J.-M., Wang, X.-Y., Nakawo, M., Xie, Z.-C., Zhang, J.-M., Zhang, X.-Z., 2010. Climatological significance of stable isotopes in precipitation over south-west China. Int. J. Climatol. 30, 2229–2239.

Zhu, H., Cao, M., Hu, H., 2006. Geological history, flora, and vegetation of Xishuangbanna, Southern Yunnan, China. Biotropica 38, 310–317.